ISSN 0023-1584, Kinetics and Catalysis, 2010, Vol. 51, No. 2, pp. 273–278. © Pleiades Publishing, Ltd., 2010.
Original Russian Text © A.V. Vishnyakov, I.A. Korshunova, V.E. Kochurikhin, L.S. Sal'nikova, 2010, published in Kinetika i Kataliz, 2010, Vol. 51, No. 2, pp. 288–294.

Catalytic Activity of Rare Earth Oxides in Flameless Methane Combustion

A. V. Vishnyakov, I. A. Korshunova, V. E. Kochurikhin, and L. S. Sal'nikova

Mendeleev University of Chemical Technology of Russia, Moscow, 125047 Russia

e-mail: irina-kk@yandex.ru

Received December 15, 2008

Abstract—The following rare earth oxides, which were prepared by the precipitation of hydroxides, were studied as catalysts for the reaction of complete methane oxidation: CeO_2, a hydrated phase of La_2O_3, Pr_6O_{11}, Tb_4O_7, and Gd_2O_3. The catalytic activities of the oxides were compared in terms of first-order reaction rate constants per unit surface area of the catalyst. With consideration for data on the reduction of CeO_2, Pr_6O_{11}, and Tb_4O_7, the previously proposed redox reaction mechanism on transition metal oxides was supported. The high activity of hydrated La_2O_3 was found, and it was hypothesized that, in this case, the process occurred by the mechanism of oxidative methane condensation followed by the rapid oxidation of the resulting intermediate products.

DOI: 10.1134/S0023158410020163

INTRODUCTION

The catalytic oxidation of methane in lean gas–air mixtures has been the subject matter of a great number of studies. Interest in this problem is explained by the fact that the oxidation of methane under standard conditions is impossible at its concentrations lower than 4%. Only catalytic combustion makes it possible to avoid the release of methane into the atmosphere. Methane is a greenhouse gas whose environmental impact is greater than the effect caused by the release of CO_2 by a factor of 20. This process is of special importance in the development of systems for CH_4 neutralization in gas mixtures released from coalmine ventilation systems. In a medium mine (with the production of about 0.5 million tons per year), the release of CH_4 is equivalent to 50000 MW in terms of energy; in this case, the environmental impact is the same as that upon the release of carbon dioxide exhausted in the operation of 500000 of automobiles into the environment.

The first step in the development of energy-efficient and environmentally safe systems for the utilization of methane released into the atmosphere from coal mining was made in Australia in 2005. A catalytic reactor for methane combustion (CH_4 concentration, 0.9%; atmospheric emission, 250000 m^3/h) combined with a water-steam gas turbine was implemented at a coalmine. Methane was oxidized on a supported Pd catalyst at 400–500°C. At higher concentrations of CH_4 (3–3.5%), the temperature in the catalytic unit where methane is combusted should be as high as 700–900°C. Under these conditions, the long-term operation of supported palladium catalysts is impossible because of catalyst degradation. Because of this, it is necessary to search for new catalysts resistant to agglomeration with high activity and developed surface area.

Unfortunately, nanosized perovskite-like catalysts, which are efficient at temperatures lower than 600°C, do not have a required set of properties at elevated temperatures [1]. Rare earth oxides can be considered among alternative thermally stable and sufficiently efficient catalysts [2, 3].

The aim of this work was to study the catalytic properties of a number of rare earth oxides (CeO_2, La_2O_3, Pr_6O_{11}, Tb_4O_7, and Gd_2O_3) in order to follow the effect of their redox and acid–base characteristics on the catalytic activity. The first-named oxide (CeO_2) is amphoteric, and it mainly contains Ce^{4+}. Praseodymium is readily reduced to a state of Pr^{3+}; therefore, it forms a mixed-valence phase of Pr_6O_{11} ($4PrO_2 + Pr_2O_3$). In the Tb_4O_7 oxide, the relative concentration of Tb^{3+} is even higher ($2TbO_2 + Tb_2O_3$). La_2O_3 exhibits pronounced basic properties, and it contains a singe charged state of La^{3+} similarly to Gd_2O_3 [4].

EXPERIMENTAL

Catalyst Synthesis

La_2O_3, CeO_2, Pr_6O_{11}, and Tb_4O_7 were synthesized from hydroxides precipitated from corresponding aqueous metal nitrate solutions by adding magnesium hydroxide. The precipitating agent was chosen for convenience. The nitrates of Pr and Tb were prepared by dissolving commercial Pr_6O_{11} and Tb_4O_7 oxides in concentrated nitric acid. The hydroxide precipitates were filtered off, thoroughly washed with water, and dried at 90–110°C for 5 h. Thereafter, they were cal-

Characteristics of rare earth oxides

Oxide	Phase (according to XRD data)	S_{sp}, m^2/g	D_a^*, nm (according to the Scherrer equation)	Concentration of Mg, wt %
La_2O_3	$La(OH)_3$, $La_2O_2CO_3$	13.3	19	0.7
CeO_2	Cubic CeO_2	17.4	19	0.1
Pr_6O_{11}	Cubic Pr_6O_{11}	8.8	26	0.9
Tb_4O_7	Cubic Tb_4O_7	8.1	16	0.6
Gd_2O_3	Cubic Gd_2O_3	2.7	28	–

* Coherent scattering region size.

cined at 475°C for 1 h and, additionally, at 775°C for 3.5 h. The concentrations of the precipitating agent in the resulting samples were determined by inductively coupled plasma atomic emission spectrometry on a Spectro Ciros Vision instrument (Germany) after transferring the samples into solution. The residual magnesium content of the materials was no higher than 1 wt %. The presence of a small amount of magnesium had no effect on the catalytic activity of the samples, as experimentally demonstrated in the tests of commercial La_2O_3, Pr_6O_{11}, and Tb_4O_7 oxides whose specific surface areas were lower than that of the synthesized catalysts by a factor of 2–3.

Commercial powdered Gd_2O_3 (China) was obtained by the thermal decomposition of oxalate (A & C Rare Earth Materials Co).

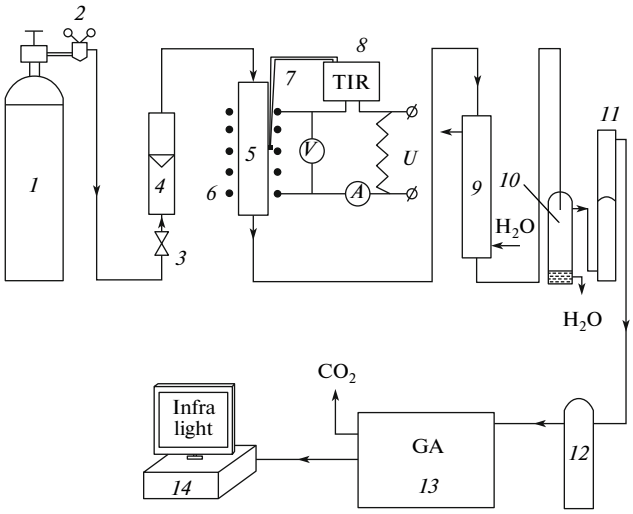

Fig. 1. Schematic diagram of the setup for testing catalysts: (*1*) cylinder with a gas mixture, (*2*) reducer, (*3*) needle valve, (*4*) rotameter, (*5*) reactor, (*6*) electric furnace, (*7*) thermocouple, (*8*) 2TRM1 temperature regulator and meter with cold junction compensation (OVEN), (*9*) condenser, (*10*) water inlet, (*11*) soap film flow meter, (*12*) foam catcher, (*13*) INFRALIGHT 11P IR gas analyzer, and (*14*) computer.

Catalyst Characterization

Specific surface areas were measured using the low-temperature adsorption of argon. X-ray diffraction (XRD) analysis was performed on a DRON-3M diffractometer (CuK_α radiation; Ni filter; λ = 0.15418 nm) over the range of 2θ from 10° to 80°. The resulting diffraction patterns were compared with data from the JCPDS data base. The XRD patterns of CeO_2, Pr_6O_{11}, Tb_4O_7, and Gd_2O_3 samples corresponded to cubic lattice parameters.

Lanthanum oxide mainly contained $La(OH)_3$ and $LaCO_3OH$ and $La_2O_2CO_3$ impurities. The presence of impurities was not associated with the procedure chosen for the production of the preparation. The XRD analysis of Russian and Chinese commercial samples demonstrated that all of them also contained the above impurities, although they were nominally characterized as La_2O_3. It is well known that the complete decomposition of lanthanum hydroxide containing carbonate impurities occurs at about 1000°C [5]. Taking into account the facts that this effect inevitably decreases the specific surface area and lanthanum oxide absorbs water vapor and CO_2 in contact with a gas atmosphere formed in the course of methane oxidation, we used a hydrated phase of lanthanum oxide, subsequently referred to as "La_2O_3," in the further experiments.

The table summarizes the above characteristics of the synthesized substances and the crystallite size D_{av} estimated from diffraction line broadening (the average value of three peaks).

Determination of Catalytic Activity

The catalytic activity of the samples was measured using a flow-type system (Fig. 1). A quartz grate covered with quartz cloth was arranged at the center of a tubular reactor 10 mm in inner diameter and 450 mm in length, and a catalyst mixed with an inert filler (crushed corundum ceramics) was placed on this cloth (1.2 g of ceramics per 200 mg of catalyst). On top, the sample was also fixed with quartz cloth. The particle sizes of the catalyst and crushed ceramics were 0.063–0.125 and 0.1–0.3 mm, respectively.

The gas mixture was supplied at a rate of 80 ml/min. The furnace temperature was stepwise increased at a step of 50°C with establishing every time a constant mixture composition at the reactor outlet. The error in the determination of temperature was ±0.1°C. The gas flow at the reactor outlet was passed through an IR gas analyzer. The detection limits of mixture components were the following: methane, 0.01%; CO, 0.001%; and CO_2, 0.01%.

Primary information on the catalytic activity of the samples was obtained as the temperature dependence of the conversion of CH_4, which was measured in the on-line regime at a fixed gas flow rate. The experiments were performed with the use of the mixtures of methane (1 or 3.3%) with "synthetic air" (N_2–O_2 in a ratio of 1 : 5). The concentration of oxygen with respect to methane was higher than a stoichiometric amount by a factor of more than 3. The kinetic curves were adequately reproduced in repeated heating–cooling cycles.

According to published data [3, 6, 7], the reaction is of first order with respect to methane and zero order with respect to oxygen. Thus, analogously to Alifanti et al. [7], we characterized the catalytic activity by the apparent rate constant of pseudo-first-order reaction per unit surface area of the catalyst:

$$k_s = \ln\left(\frac{1}{1-\alpha}\right)\frac{V}{PmS_{sp}}, \quad (1)$$

where V is the gas mixture flow rate in μmol/s; P is the total pressure in the system in atm; α is the conversion of CH_4; m is the catalyst weight in g; and S_{sp} is the specific surface area of the sample in m^2/g.

The similarity of reaction rate constants (error of no higher than 8%) in experiments with different catalyst weights (200 and 400 mg) and various gas flow rates (from 80 to 240 ml/min) demonstrates that the calculation procedure was adequately chosen and external diffusion inhibition was absent.

The constancy of the catalytic activity of the samples was evaluated by analyzing the dependence of methane conversion on reaction time (up to 50 h) at the temperature that ensured the maximum starting methane conversion (as a rule, 98–100%).

To get a notion of the dependence of the temperature of the onset of methane oxidation on catalyst reduction conditions, we studied the interaction of the catalysts with hydrogen or methane under temperature-programmed reaction conditions. In the former case, a ceramic container with a weighed portion of an oxide was loaded in the reactor; air was evacuated from the system, and hydrogen was added to a specified pressure. Changes in the pressure of H_2 were measured using a deformation membrane gage from Vernier (United States). Then, the reactor with the container was placed in a furnace, and a compressor was turned on for producing gas circulation. The temperature was increased at a step of 8–10 K/min (over a range from 250 to 750°C), and changes in the pressure of hydrogen were measured in the course of the experiment.

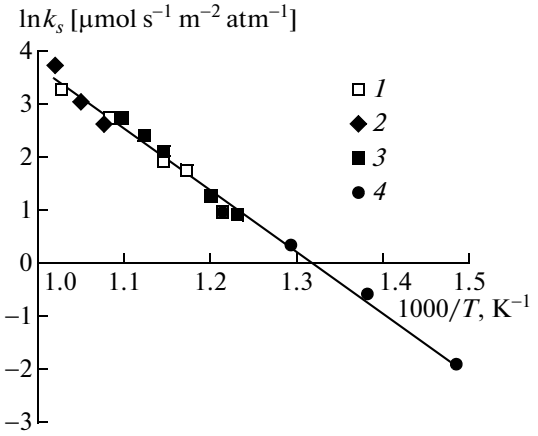

Fig. 2. The temperature dependence of the rate constant of the reaction: (*1*) this work (CeO_2 prepared by hydroxide decomposition at 775°C; S_{sp} = 17.4 m^2/g), (*2*) published data [3] (carbonate decomposition at 650°C; S_{sp} = 28 m^2/g), (*3*) published data [8] (cerium citrate decomposition at 700°C; S_{sp} = 21 m^2/g), and (*4*) published data [10] (commercial sample; S_{sp} = 79 m^2/g).

The degree of oxide reduction in methane was evaluated from a decrease in CH_4 in contact with the catalyst and from an increase in the concentration of CO_2. The gas mixture contained 1% methane and 99% helium. The furnace temperature was stepwise increased at a step of 50°C.

RESULTS AND DISCUSSION

Among the oxides examined, only the catalytic activity of cerium dioxide in the reaction of methane oxidation was measured in a number of studies [3, 8–10]. Therefore, it is reasonable to begin the consideration of the results obtained in this work with this oxide. A comparison with available independent data suggests that the procedures used for testing the catalytic activity and processing the experimental results were reliable.

As expected, the activity of CeO_2 was low: the conversion of methane was as low as 83% even at 750°C. In a quasi-first-order approximation, the temperature dependence of methane conversion was linearized in the Arrhenius coordinates ($\ln k_s$–$1/T$) over the range of CH_4 conversions from 10 to 90% (Fig. 2). Figure 2 also includes published data.

As can be seen, our results are consistent with published data [3, 8, 10], although there are considerable differences in the specific surface areas and methods of sample synthesis. The combined treatment of all of these data over a temperature range of 400–700°C resulted in the equation

$$\ln k_s = 11600/T + 15.3. \quad (2)$$

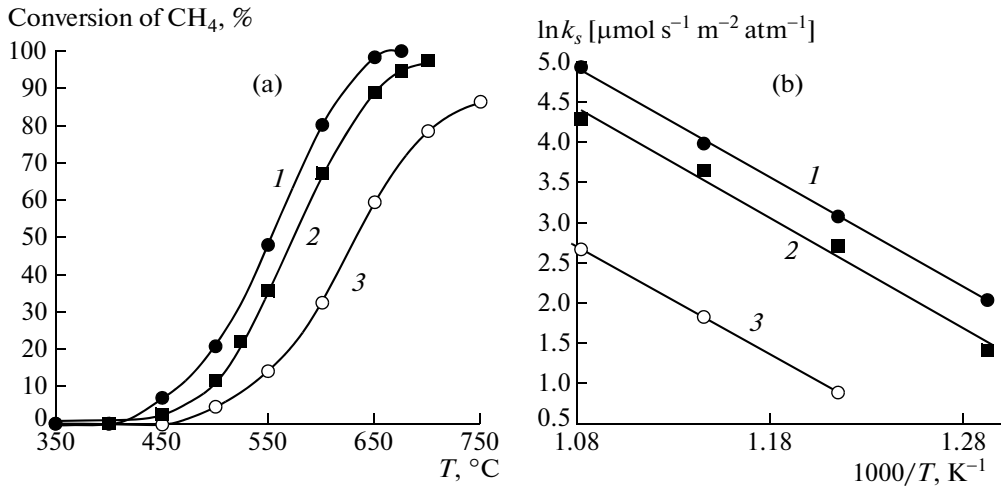

Fig. 3. The temperature dependence of (a) the extent of CH_4 oxidation and (b) the rate constant of the reaction: (*1*) Pr_6O_{11} (S_{sp} = 8.8 m^2/g), (*2*) Tb_4O_7 (S_{sp} = 8.1 m^2/g), and (*3*) CeO_2 (S_{sp} = 17.4 m^2/g).

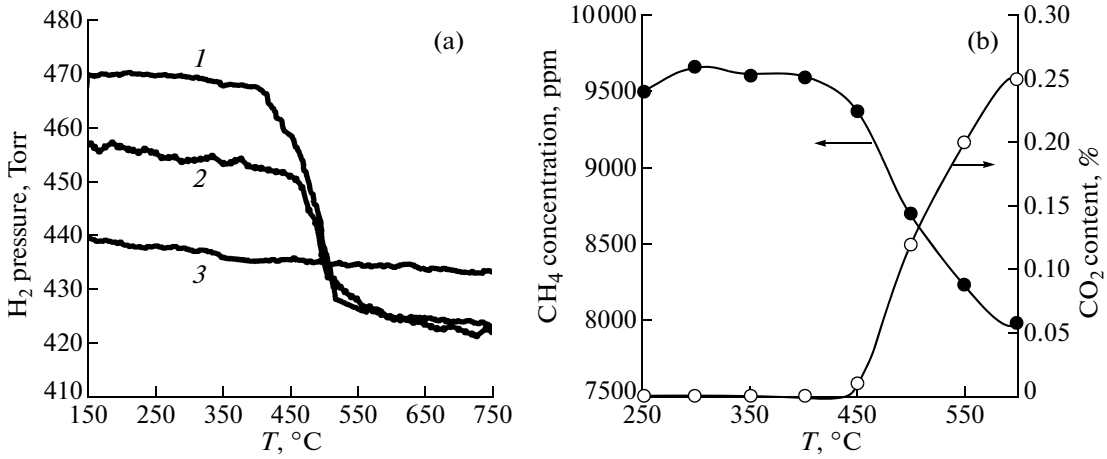

Fig. 4. The reduction of (a) (*1*) Pr_6O_{11}, (*2*) Tb_4O_7, and (*3*) CeO_2 in hydrogen and (b) Pr_6O_{11} in methane.

Unlike CeO_2, the mixed-valence Pr_6O_{11} and Tb_4O_7 oxides exhibited much higher activity (Fig. 3). For example, the conversion of methane on Pr_6O_{11} was as high as 90% even at 623°C.

The apparent activation energy increased insignificantly but monotonically from 103 kJ/mol on CeO_2 to 108 or 112 kJ/mol on Pr_6O_{11} or Tb_4O_7, respectively. Error in the determination of E_a was 4–6%; it mainly depended on the accuracy of temperature control in the course of the experiment [11].

Pr_6O_{11} and Tb_4O_7 retained their initial activities (conversions of 100 and 98%, respectively) for at least 20 h at 750°C.

A decrease in the stability of a state of Ln^{4+} may be the most probable reason for a dramatic increase in the catalytic activity on going from cerium oxide to praseodymium oxide. It is well known that the amount of oxygen released upon the dissociation of Pr_6O_{11} and Tb_4O_7 was greater by several orders of magnitude than that upon the decomposition of CeO_2.

These data are fully consistent with the results of our experiments on the temperature-programmed reduction of the above oxides in an atmosphere of hydrogen and methane. Unlike the mixed-valence oxides of Pr and Tb, CeO_2 did almost not absorb hydrogen at temperatures lower than 500°C. At the same time, the reduction of Pr_6O_{11} and Tb_4O_7 began at 400 and 450°C, respectively (Fig. 4). An analogous behavior was observed in the interaction of Pr_6O_{11} with methane. Note that the oxidation of methane on praseodymium and terbium oxides began at temperatures that almost coincided with the temperature of the onset of their reduction with hydrogen and methane to metal(III) oxides (~450°C).

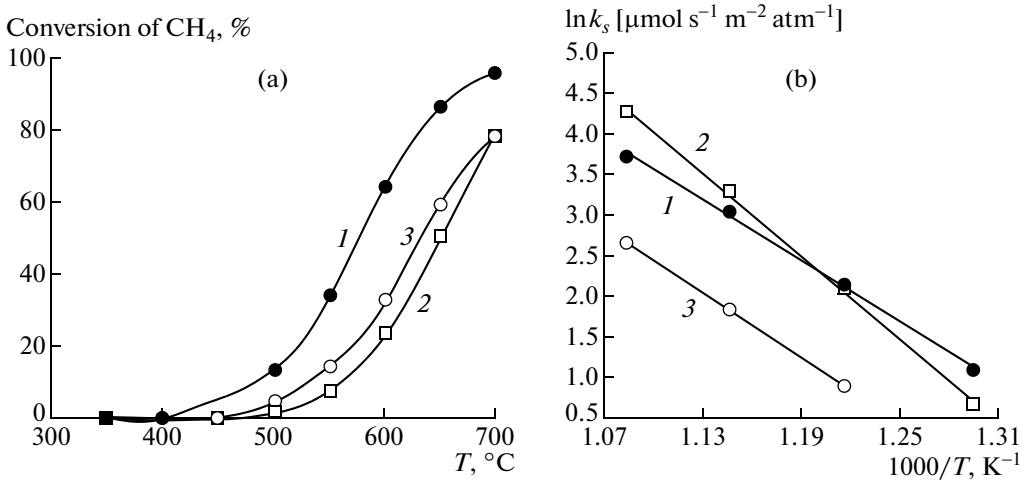

Fig. 5. The temperature dependence of (a) the extent of CH_4 oxidation and (b) the rate constant k_s on the following catalysts: (*1*) "La_2O_3" (S_{sp} = 13.3 m^2/g), (*2*) Gd_2O_3 (S_{sp} = 2.7 m^2/g), and (*3*) CeO_2 (S_{sp} = 17.4 m^2/g).

The above results allowed us to conclude that the oxidation of CH_4 on Pr_6O_{11} and Tb_4O_7 occurs by a so-called redox mechanism [7, 8]:

$$(1)\ H_3C{-}H + [O][M^{n+}O_m]$$
$$\longrightarrow [H_3\dot{C}] + [OH][M^{n+}O_m];$$
$$(2)\ [H_3\dot{C}] + [M^{n+}O_m][OH]$$
$$\longrightarrow [M^{(n-1)+}O_{m-3}\,CO_2] + 2[H_2O];$$
(3) desorption of H_2O and CO_2 (slow step);
$$(4)\ [M^{(n-1)+}O_{m-3}] + 2O_2 \longrightarrow [O]\,[M^{n+}O_m].$$

An important prerequisite for this mechanism is the occurrence of oxide transition metal (M^{n+}) constituents capable of changing their charge state at step 1 and undergoing the oxidation of a reduced form at step 4 in contact with oxygen, which was present in an excess in the reaction mixture.

Because Ln^{3+} is the only possible charge state for the majority of rare earth oxides, it was hard to expect that La_2O_3 and Gd_2O_3 will efficiently catalyze methane oxidation in accordance with the above mechanism of the catalytic oxidation of methane. Indeed, it was found that hydrated lanthanum oxide ("La_2O_3") was close to Tb_4O_7 in activity (Fig. 5). The test of the stability of La_2O_3 at 700°C demonstrated that the sample retained its activity (98.5% conversion) for 20 h.

To interpret the behavior of "La_2O_3," let us consider simultaneously the following sets of data:

• data on the thermal stability of lanthanum hydroxide, which began to decompose at 550–600°C according to published data [12, 13];

• data on the temperature dependence of the rate of the thermal dissociation of lanthanum, neodymium, and gadolinium oxy carbonates $Ln_2O_2CO_3 \longrightarrow Ln_2O_3 + CO_2$ [14, 15];

• data on the partial pressure of CO_2 in a gas phase (the $CH_4{-}CO_2{-}H_2O{-}O_2{-}N_2$ system), which initially contained 1% methane, over various catalysts as the temperature was increased from 400 to 700°C.

Figure 6 illustrates all of the above data. As can be seen, the partial pressure of CO_2 in the gas atmosphere in contact with "La_2O_3" was higher than the dissociation pressure of oxo carbonate at temperatures lower than 660°C. Thus, both lanthanum oxide and lanthanum hydroxide would be converted into $La_2O_2CO_3$ in contact with a $CH_4{-}CO_2{-}H_2O{-}O_2{-}N_2$ gas mixture formed as a result of methane oxidation. Above 660°C, the dissociation pressure of $La_2O_2CO_3$ was higher than the pressure of CO_2; that is, conditions were produced under which the thermal dissociation of the resulting

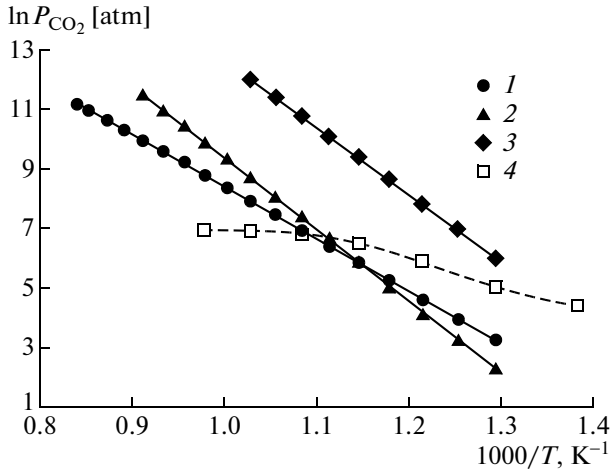

Fig. 6. The temperature dependence of the partial pressure of CO_2 in the dissociation of the oxocarbonates (*1*) $La_2O_2CO_3$ [14], (*2*) $Nd_2O_2CO_3$ [15], and (*3*) $Gd_2O_2CO_3$ [15] and (*4*) in the oxidation of methane on "La_2O_3."

oxo carbonate became possible. However, this did not change the character of the dependence of $\ln k_s$ on $1/T$. Hence, it follows that either lanthanum oxide and oxo carbonate phases in combination or a lanthanum oxide and oxo carbonate phase as a solid solution can catalyze the process at temperatures higher than 660°C.

An analysis of published and patented data indicated that La_2O_3 and $La_2O_2CO_3$ belong to the most effective catalysts for the oxidative coupling of methane (OCM), which results in the formation of ethane, propane, ethylene, propylene, H_2O, and CO_2 as the main products [16–21]. Usually, OCM is considered as a side process accompanying the oxidation of methane in the mixtures of CH_4 with O_2 in an excess of methane. The OCM reaction on La_2O_3 and $La_2O_2CO_3$ begins in the temperature range of 400–450°C [17–21], which almost coincides with the temperature of the onset of CH_4 oxidation on "La_2O_3." It is also well known that the complete oxidation of ethane and ethylene occurs at a higher rate than the oxidation of methane and it comes into play at a noticeably lower temperature. Thus, if the oxidation of CH_4 involves the step of catalytic condensation, all of the resulting hydrocarbons will be oxidized in an excess of oxygen to CO_2 and H_2O at temperatures higher than 450°C, and they cannot be detected among the reaction products. It is reasonable to assume that this oxidation mechanism can be extended to other "light group" rare earth oxides with pronounced basic properties (Sm, Nd).

Gadolinium oxide forms a stable hydroxide similarly to La_2O_3 [22]. Therefore, it is believed that the oxidation of methane on Gd_2O_3 also occurs by the oxidative condensation mechanism. However, unlike lanthanum oxide, Gd_2O_3 does not form stable oxo carbonates. According to published data (see Fig. 6), gadolinium oxo carbonate begins to decompose at temperatures higher than 300°C; that is, it cannot be formed in contact with a gas mixture under conditions of methane oxidation for thermodynamic reasons. It is likely that because of this the apparent activation energy of CH_4 oxidation on Gd_2O_3 is much higher than that on La_2O_3 (130 and 112 kJ/mol, respectively).

Thus, in the course of this study, we obtained data on the flameless combustion of methane on the rare earth oxides CeO_2, Pr_6O_{11}, Tb_4O_7, and Gd_2O_3 and a hydrated La_2O_3 phase. The catalytic activity was evaluated in terms of the rate constant of quasi-first-order reaction per unit surface area of the catalyst. It is believed that the oxidation of methane on CeO_2, Pr_6O_{11}, and Tb_4O_7 occurred in accordance with a redox mechanism, and the oxidation on hydrated La_2O_3 occurred by the mechanism of oxidative CH_4 condensation followed by the rapid oxidation of the resulting intermediate products.

REFERENCES

1. Chiarello, G.L., Rossetti, I., Forni, L., Lopinto, P., and Migliavacca, G., *Appl. Catal., B*, 2007, vol. 72, p. 218.
2. Boreskov, G.K., *Kataliz: Voprosy teorii i praktiki* (Catalysis: Theory and Practice), Novosibirsk: Nauka, 1987, p. 536.
3. Liu, W. and Flytzani-Stephanopoulos, M., *J. Catal.*, 1995, vol. 153, p. 304.
4. Adachi, G., Nobuhito, I., and Kang, Z.C., *Binary Rare Earth Oxides*, Dordrecht: Kluwer, 2004, p. 10.
5. US Patent 6733882.
6. Vishnyakov, A.V., Kryukov, A.Yu., Chashchin, V.A., and Golosman, E.Z., *Khim. Prom–st. Segodnya*, 2007, no. 4, p. 15.
7. Alifanti, M., Kirchnerova, J., and Delmon, B., *Appl. Catal., A*, 2003, vol. 245, p. 231.
8. Kirchnerova, J., Alifanti, M., and Delmon, B., *Appl. Catal., A*, 2002, vol. 231, p. 65.
9. Kundakovic, Lj. and Flytzani-Stephanopoulos, M., *J. Catal.*, 1998, vol. 179, p. 203.
10. Liotta, L.F., Di Carlo, G., Pantaleo, G., and Deganello, G., *Catal. Commun.*, 2005, vol. 6, p. 329.
11. Benson, S.W., *The Foundations of Chemical Kinetics*, New York: McGraw-Hill, 1960.
12. Portnoi, K.I. and Timofeeva, N.I., *Kislorodnye soedineniya redkozemel'nykh elementov* (Oxide Compounds of Rare-Earth Metals), Moscow: Metallurgiya, 1986.
13. Neumann, A. and Walter, D., *Thermochim. Acta*, 2006, vol. 445, p. 200.
14. Shirsat, A.N., Ali, M., Kaimal, K.N.G., Bharadwaj, S.R., and Das, D., *Thermochim. Acta*, 2003, vol. 399, p. 167.
15. Shirsat, A.N., Kaimal, K.N.G., Bharadwaj, S.R., and Das, D., *J. Phys. Chem. Solids*, 2005, vol. 66, p. 1122.
16. US Patent 6518476.
17. Kus, S., Otremba, M., and Taniewski, M., *Fuel*, 2003, vol. 82, p. 1331.
18. US Patent 6576803.
19. Dedov, A.G., Loktev, A.S., Moiseev, I.I., Aboukais, A., Lamonier, J.-F., and Filimonov, I.N., *Appl. Catal., A*, 2003, vol. 245, p. 209.
20. US Patent 6403523.
21. US Patent 4929787.
22. Chang, Ch. and Mao, D., *Int. J. Chem. Kinet.*, 2006, vol. 39, no. 2, p. 75.